

Macrocyclic $[M_2L(\mu-L')]^+$ Complexes ($M = Ni^{II}, Zn^{II}$; $L' = Cl^-$ or RCO_2^-) Incorporating Thiophenolate and Phenylsulfonate Donor Units: Preparation, Reactivity, Structure, and Stability

Steffen Käss^[a] and Berthold Kersting^{*[a]}

Keywords: Nickel / Zinc / Macrocyclic ligands

The effect of *de-tert*-butylation on the coordinating properties of the 24-membered hexaazadithiophenolate macrocycle 13,27-bis(*tert*-butyl)-3,6,9,17,20,23-hexaazatricyclo-[23.3.1.11.15]triaconta-1(28),11,13,15(30),25,26-hexaene-29,30-dithiol (H_2L^1) has been examined. For this purpose, a series of mixed-ligand Ni^{II} and Zn^{II} complexes of the *de-tert*-butylated hexaaminedithiophenolate macrocycle H_2L^2 were prepared and characterized, namely, $[Ni^{II}_2L^2(Cl)]^+$ (**1b**), $[Zn^{II}_2L^2(OAc)]^+$ (**2b**), $[Ni^{II}_2L^2(O_2CCH=CHPh)]^+$ (**3b**), $[Zn^{II}_2L^2(O_2CCH=CHPh)]^+$ (**4b**), $[Ni^{II}_2L^2(O_2CC_{14}H_{17})]^+$ (**5b**), $[Zn^{II}_2L^2(O_2CC_{14}H_{17})]^+$ (**6b**, in which $C_{14}H_{17}CO_2^- = 3,4$ -dimethyl-6-phenylcyclohex-3-enecarboxylate), $[Ni^{II}_2L^2(O_2CC_6H_4-3-OMe)]^+$ (**7b**), and $[Zn^{II}_2L^2(O_2CC_6H_4-3-OMe)]^+$ (**8b**). The synthesis and characterization data for complexes $[Ni^{II}_2L^4(O_2CC_6H_4-3-OMe)]^+$ (**7d**) and $[Zn^{II}_2L^4(O_2CC_6H_4-3-OMe)]^+$ (**8d**), in which H_2L^4 represents the *S*-oxygenated (bis-sulfonate) derivative of H_2L^2 are also reported. The *de-tert*-butylated macrocycles H_2L^2 (and H_2L^4) behave essen-

tially in the same fashion as H_2L^1 (and H_2L^3) producing dinuclear mixed-ligand $[M_2L(\mu-L')]^+$ complexes with analogous bioctahedral core structures in similar good yields and reaction times. The spectroscopic features of the $[M_2L^2(\mu-L')]^+$ and $[M_2L^4(\mu-L')]^+$ complexes resemble those of the analogous complexes supported by the *tert*-butylated derivatives H_2L^1 and H_2L^3 . One major difference between the $[M_2L^{1,3}(\mu-L')]^+$ and $[M_2L^{2,4}(\mu-L')]^+$ complexes concerns the depth of the binding pocket of the compounds, which is significantly reduced upon removing the *tert*-butyl substituents. Another significant difference associated with removal of the *tert*-butyl substituent concerns the less pronounced differences of the relative stability constants for the carboxylato-bridged $[M_2L^2(\mu-O_2CR)]^+$ complexes (as compared to the $[M_2L^1(\mu-O_2CR)]^+$ complexes). These stability differences can be qualitatively explained in terms of less pronounced intramolecular $CH\cdots\pi$ and/or van der Waals interactions in the *de-tert*-butylated complex systems.

Introduction

The coordination chemistry of Robson-type polyaza-dithiophenolate ligands has been actively investigated over the past several years,^[1–3] because they are ideally suited as supporting ligands for the preparation of model compounds for dinuclear metalloenzymes,^[4] for the stabilization of unusual metal oxidation states,^[5] and to understand, achieve, and control dinuclear metal reactivity.^[6,7]

We have investigated the coordination chemistry of the octadentate hexaaza-dithiophenolate ligand H_2L^1 in much detail (Figure 1). The specific feature of H_2L^1 is its capsular, cleftlike structure reminiscent of the “cone” conformation of the calixarenes^[8] that it adopts in its mixed-ligand complexes of composition $[M^{II}_2L^1(\mu-L')]^+$, in which L' is the coligand and M^{II} a first-row transition-metal ion.^[9,10] This conformation of $(L^1)^{2-}$ provides a deep binding cavity that considerably influences the complex stability^[11,12] and reactivity.^[13,14]

The unique reactivity features of these complexes^[15,16] led us to investigate potential routes to derivatives of H_2L^1

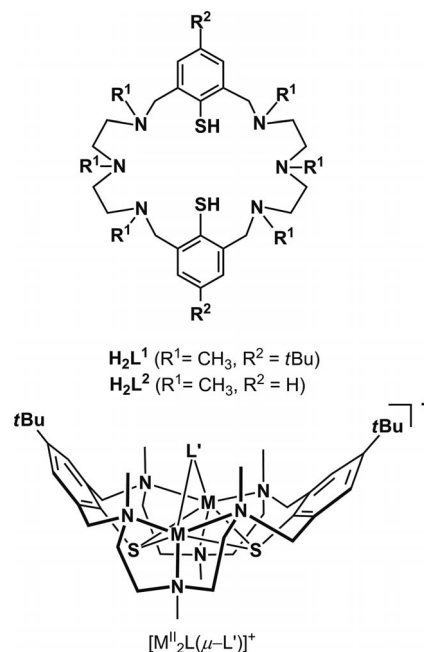


Figure 1. Top: Structure of the ligands H_2L^1 and H_2L^2 . Bottom: Perspective view of the structure of complexes of the type $[M_2L^1(\mu-L')]^+$.

[a] Institut für Anorganische Chemie, Universität Leipzig,
04103 Leipzig, Germany
Fax: +49-341-973-6199
E-mail: b.kersting@uni-leipzig.de

that would provide more rigid and deeper binding cavities, and many variants have now been prepared. The modifications included alteration of the *N*-methyl functions by substituents sterically more demanding than a methyl group (e.g., $R^1 = \text{Et}, \text{Pr}$),^[17] installation of different *N*-alkyl groups on the benzylic and central nitrogen atoms of the linking diethylenetriamine units,^[18] incorporation of pendant donor R^1 arms,^[19] elongation of the diethylenetriamine linker groups,^[20] and *S*-oxygenation of the thiophenolate sulfur atoms.^[21,22] More recently, we have also been able to alter the R^2 substituents in the *para* position to the thiophenolate sulfur atoms (e.g., $R^2 = \text{H}, \text{Ph}, 4\text{-}t\text{Bu-Ph}$).^[16,23]

This study focuses on the ligand H_2L^2 , which represents the *de-tert*-butylated derivative of the parent ligand H_2L^1 . We have prepared eight Ni^{II} and Zn^{II} complexes of the ligand (L^2)²⁻ bearing Cl^- and various RCO_2^- coligands **1b–8b** (see Figure 2). Their properties are compared with the analogous $[\text{M}_2\text{L}^1(\mu\text{-L}')]^+$ complexes **1a–6a** to establish whether the choice of the substituent in the *para* position of the thiophenolate head unit affects the structures and properties of the complexes. The characterization of the new compounds **7d** and **8d**, obtained by oxidation of **7b** and **8b**, respectively, is also reported.

Results and Discussion

Preparation of the Ligands and Metal Complexes

The aminothiophenolate ligand H_2L^2 was synthesized from 2-bromo-1,3-dimethylbenzene by a multistep procedure as described in the literature.^[16] The macrocycle was isolated as the hexahydrochloride salt and stored under a protective argon atmosphere due to its air sensitivity. The synthesized complexes and their labels are depicted in Figure 2. All complexes of the *de-tert*-butylated macrocycle H_2L^2 are reported for the first time except **2b**.^[16] The metal complexes supported by H_2L^1 , namely, the chlorido- (**1a**),^[24] acetato- (**2a**),^[25] cinnamato- (**3a, 4a**), and 3,4-dimethyl-6-phenylcyclohex-3-enecarboxylato-bridged (**5a, 6a**) Ni^{II} and Zn^{II} complexes,^[16] on the other hand, have all been reported previously and serve here merely as reference compounds.

Complexes $[\text{Ni}_2\text{L}^2(\text{Cl})]^+$ (**1b**) and $[\text{Zn}_2\text{L}^2(\text{OAc})]^+$ (**2b**) were readily obtained from stoichiometric complexation reactions between the free ligand $\text{H}_2\text{L}^2 \cdot 6\text{HCl}$ and nickel(II) chloride hexahydrate or zinc(II) acetate dihydrate, respectively, in the presence of a solution of triethylamine in methanol (Scheme 1), followed by isolation as perchlorate salts.

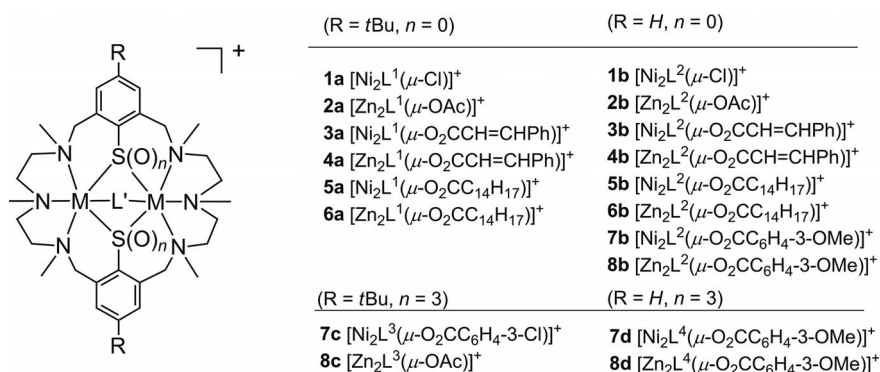
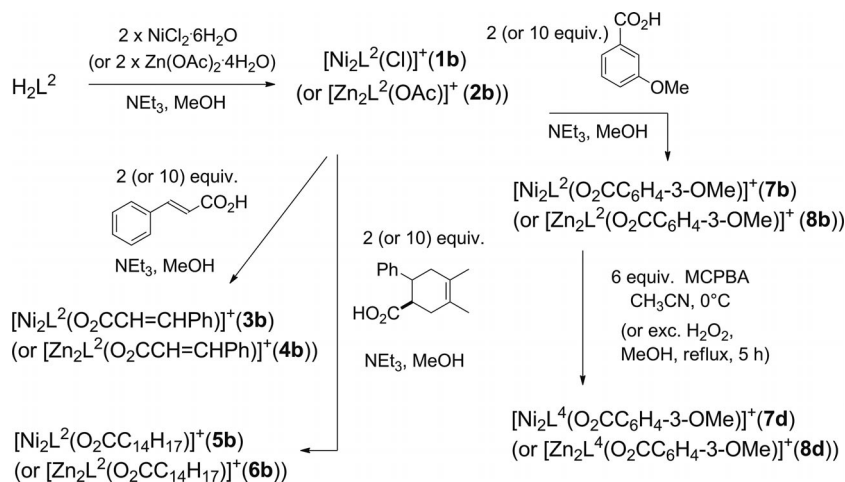


Figure 2. Complexes studied in this work ($\text{C}_{14}\text{H}_{17}\text{CO}_2^- = 3,4\text{-dimethyl-6-phenylcyclohex-3-enecarboxylate}$)^[26].



Scheme 1. Synthesis of the $[\text{M}_2\text{L}^2(\mu\text{-L})]^+$ and $[\text{M}_2\text{L}^4(\mu\text{-L})]^+$ complexes **1b–8d** ($\text{C}_{14}\text{H}_{17}\text{CO}_2^- = 3,4\text{-dimethyl-6-phenylcyclohex-3-enecarboxylate}$).

The latter were subjected to salt metathesis with NaBPh_4 to generate the corresponding tetraphenylborate salts. The complexation reactions appear to be unaffected by the choice of supporting ligand. The *de-tert*-butylated macrocycle H_2L^2 reacts essentially in the same fashion as H_2L^1 producing dinuclear mixed-ligand $[\text{M}_2\text{L}(\mu\text{-L}')^+]^+$ complexes with analogous structures in similar good yields and reaction times.^[17,27] The solubilities of **1b** and **2b** resemble those of **1a** and **2a**.

To obtain further pairs of analogous complexes supported by $(\text{L}^1)^{2-}$ and $(\text{L}^2)^{2-}$, substitution reactions of **1b** and **2b** were performed. Cinnamate and 3,4-dimethyl-6-phenylcyclohex-3-enecarboxylate were selected as coligands (Scheme 1). Treatment of the chlorido-bridged complex **1b** with a slight excess amount of the corresponding triethylammonium carboxylate in methanol at ambient temperature over the course of 2 h provided the carboxylato-bridged Ni_2 complexes **3b** and **5b** in almost quantitative yield. It should be noted that these reactions are not simple substitution reactions, because a simultaneous conformational change of the supporting ligand (from structure type A present in **1b** to type B in **3b** and **5b**) takes place (Figure 3). A similar behavior has been observed for complexes of H_2L^1 .^[18,28] This macrocycle adopts the bowl-shaped conformation (type B) when L' is a large monoatomic (e.g., S^{2-} , SH^-) or a multiatom bridging ligand (e.g., RCO_2^-).^[11,18] The change of the conformation can be traced back to a more favorable, less distorted octahedral coordination environment about the Ni^{2+} ions.^[29]

The bridging acetate ion in the dizinc complex **2b** could be replaced by cinnamate and 3,4-dimethyl-6-phenylcyclohex-3-enecarboxylate ions as well to give complexes **4b** and **6b**; however, a 10-fold excess amount of the entering carboxylate had to be used to drive these equilibrium reactions to completion. Again, the reactivity of **2b** is not markedly different from that of **2a**.^[16]

Included in this study are the preparation and characterization data of the 3-methoxybenzoato-bridged complexes $[\text{M}_2\text{L}^2(\text{O}_2\text{CC}_6\text{H}_4\text{-3-OMe})^+]^+$ [$\text{M} = \text{Ni}$ (**7b**); $\text{M} = \text{Zn}$ (**8b**)] and their oxidized derivatives $[\text{M}_2\text{L}^4(\text{O}_2\text{CC}_6\text{H}_4\text{-3-OMe})^+]^+$ [$\text{M} = \text{Ni}$ (**7d**); $\text{M} = \text{Zn}$ (**8d**)]. The thiophenolate complexes **7b** and **8b** were obtained by substitution reactions between 3-methoxybenzoate and **1b** or **2b**, respectively, using similar reac-

tion conditions to those given above. Conversion of the thiophenolate head units in **7b** to phenylsulfonate groups in **7d** was carried out in analogy to a previously described method.^[21] Thus, reaction of **7b** with six equivalents of *meta*-chloroperoxybenzoic acid (MCPBA) at 0 °C in MeCN generates a pale green solution, from which the lime-green sulfonato complex **7d** can be isolated as its ClO_4^- salt in excellent yields (83%). It is worth noting that the 3-methoxybenzoate coligand is not exchanged for the *meta*-chlorobenzoate ion (which stems from the MCPBA) under these conditions. It is indicative of a high kinetic inertness of the aminothiophenolate complex **7b** and implies also that all six *S*-oxygenation steps are not accompanied by complex disintegration. The oxidation of $[\text{Zn}_2\text{L}^2(\text{O}_2\text{C-C}_6\text{H}_4\text{-3-OMe})^+]^+$ (**8b**) with MCPBA produces a product mixture containing $[\text{Zn}_2\text{L}^4(\text{O}_2\text{C-C}_6\text{H}_4\text{-3-OMe})^+]^+$ (**8d**) and $[\text{Zn}_2\text{L}^4(\text{O}_2\text{C-C}_6\text{H}_4\text{-3-Cl})^+]^+$ (by NMR spectroscopy), the latter being produced by carboxylate exchange reactions with the *meta*-chlorobenzoate stemming from the MCPBA. Attempts to purify this mixture failed. However, when MCPBA was replaced by H_2O_2 , the pure compound could be isolated as its perchlorate salt in 40% yield.

All complexes are stable in air, both in solution and in the solid state. They exhibit good solubility in polar aprotic solvents such as acetonitrile, acetone, and dichloromethane, but are not very soluble in alcohols and are virtually insoluble in water. The compounds gave satisfactory elemental analyses and were characterized by spectroscopic methods (IR, UV/Vis, ^1H and ^{13}C NMR spectroscopy) and compounds **5b** and **7d** also by X-ray crystallography.

Spectroscopic Characterization of the Metal Complexes

Infrared Spectroscopy

FT infrared spectra of the dinuclear complexes were recorded over the 4000–400 cm^{-1} range. Assignments of the bands are based on comparisons between the individual complexes and on comparisons with the IR data for the respective sodium carboxylates. Table 1 lists selected spectroscopic data. The corresponding data for analogous complexes – if available – are included for comparison.^[12]

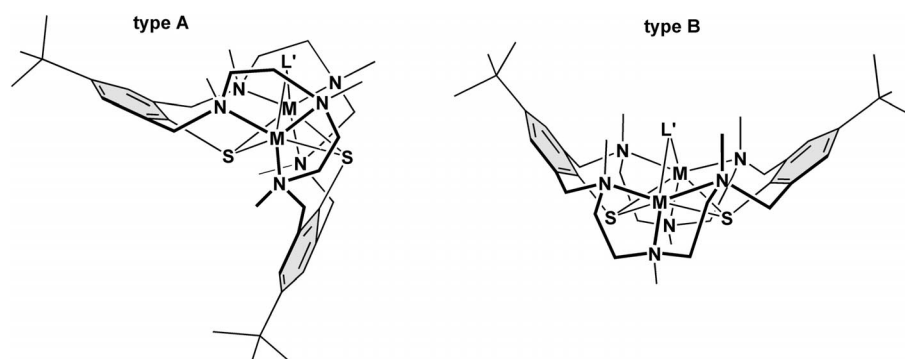


Figure 3. Schematic representation of the two macrocycle conformations A and B in mixed-ligand $[\text{Ni}_2\text{L}^1(\mu\text{-L}')^+]^+$ and $[\text{Ni}_2\text{L}^2(\mu\text{-L}')^+]^+$ complexes.^[18]

Table 1. Selected spectroscopic data for compounds **1a–8d**.^[a]

Complex	$\nu_{\text{as}}, \nu_{\text{s}}, \Delta$ [cm^{-1}] ^[b]	λ_{max} [nm] (ϵ [$\text{M}^{-1} \text{cm}^{-1}$]) ^[c]	Ref.
$[\text{Ni}_2\text{L}^1(\text{Cl})]^+$ (1a)	–	658 (41), 920 sh (59), 1002 (80)	[18]
$[\text{Ni}_2\text{L}^2(\text{Cl})]^+$ (1b)	–	662 (27), 920 sh (45), 1007 (62)	this work
$[\text{Zn}_2\text{L}^1(\text{OAc})]^+$ (2a)	1585, 1428, 157	–	[16]
$[\text{Zn}_2\text{L}^2(\text{OAc})]^+$ (2b)	1583, 1433, 150	–	this work
$[\text{Ni}_2\text{L}^1(\text{O}_2\text{CCH}=\text{CHPh})]^+$ (3a)	1578, 1406, 172	654 (27), 907 sh (40), 1125 (62)	[12]
$[\text{Ni}_2\text{L}^2(\text{O}_2\text{CCH}=\text{CHPh})]^+$ (3b)	1577, 1406, 171	658 (33), 908 sh (45), 1123 (69)	this work
$[\text{Zn}_2\text{L}^1(\text{O}_2\text{CCH}=\text{CHPh})]^+$ (4a)	1568, 1402, 166	–	[16]
$[\text{Zn}_2\text{L}^2(\text{O}_2\text{CCH}=\text{CHPh})]^+$ (4b)	1570, 1401, 169	–	this work
$[\text{Ni}_2\text{L}^1(\text{O}_2\text{CC}_{14}\text{H}_{17})]^+$ (5a) ^[d]	1573, 1400, 173	650 (29), 910 sh (29), 1112 (66)	[16]
$[\text{Ni}_2\text{L}^2(\text{O}_2\text{CC}_{14}\text{H}_{17})]^+$ (5b) ^[d]	1575, 1409, 166	650 (33), 909 sh (40), 1113 (61)	this work
$[\text{Zn}_2\text{L}^1(\text{O}_2\text{CC}_{14}\text{H}_{17})]^+$ (6a) ^[d]	1571, 1403, 168	–	[16]
$[\text{Zn}_2\text{L}^2(\text{O}_2\text{CC}_{14}\text{H}_{17})]^+$ (6b) ^[d]	1573, 1408, 165	–	this work
$[\text{Ni}_2\text{L}^2(\text{O}_2\text{CC}_6\text{H}_4\text{-3-OMe})]^+$ (7b)	1574, 1399, 175	650 (20), 909 sh (38), 1120 (45)	this work
$[\text{Zn}_2\text{L}^2(\text{O}_2\text{CC}_6\text{H}_4\text{-3-OMe})]^+$ (8b)	1570, 1399, 171	–	this work
$[\text{Ni}_2\text{L}^3(\text{O}_2\text{CC}_6\text{H}_4\text{-3-Cl})]^+$ (7c)	1563, 1410, 153	400 (47), 674 (14), 1126 (15)	[21]
$[\text{Ni}_2\text{L}^4(\text{O}_2\text{CC}_6\text{H}_4\text{-3-OMe})]^+$ (7d)	1567, 1402, 165	400 (36), 678 (9), 1132 (12)	this work
$[\text{Zn}_2\text{L}^3(\text{O}_2\text{CCH}_3)]^+$ (8c)	[1239 $\nu_{\text{s}}(\text{RSO}_3^-)$] 1595, 1411, 184	–	[21]
$[\text{Zn}_2\text{L}^4(\text{O}_2\text{CC}_6\text{H}_4\text{-3-OMe})]^+$ (8d)	[1202 $\nu_{\text{s}}(\text{RSO}_3^-)$] 1567, 1400, 167	–	this work
	[1238 $\nu_{\text{s}}(\text{RSO}_3^-)$]		

[a] The complexes were isolated as ClO_4^- and BPh_4^- salts. [b] The data correspond to the ClO_4^- salts (see the Experimental Section for the data of the BPh_4^- salts); $\Delta = \nu_{\text{as}} - \nu_{\text{s}}$. [c] Solvent: CH_3CN ; concentration: approximately 10^{-3} M. [d] $\text{C}_{14}\text{H}_{17}\text{CO}_2^- = 3,4\text{-dimethyl-6-phenylcyclohex-3-enecarboxylate}$.

The IR spectra of the chlorido-bridged complexes **1a**^[24] and **1b** are almost superimposable. However, complex **1b** exhibits an additional band at 773 cm^{-1} that can be attributed to a $\delta(\text{CH})$ bending vibration of a 1,2,3-trisubstituted arene ring.^[30] The asymmetric [$\nu_{\text{as}}(\text{CO})$] and symmetric stretching [$\nu_{\text{s}}(\text{CO})$] frequencies and their separation $\Delta [= \nu_{\text{as}}(\text{CO}) - \nu_{\text{s}}(\text{CO})]$ can be used as spectroscopic probes to identify the carboxylate binding mode.^[31–33] In the present study, the $\nu_{\text{as}}(\text{CO})$ stretching frequencies are observed in a narrow range ($1583\text{--}1567 \text{ cm}^{-1}$) as are the $\nu_{\text{s}}(\text{CO})$ frequencies ($1428\text{--}1399 \text{ cm}^{-1}$). The carboxylate stretching frequencies of the complexes supported by $(\text{L}^2)^{2-}$ are very similar to those supported by $(\text{L}^1)^{2-}$, which is indicative of a common $\mu_{1,3}\text{-RCO}_2^-$ bridging mode.^[34,35] The infrared spectrum of **7d** displays a strong band at 1239 cm^{-1} , a value typical for a sulfonate group [$\nu(\text{RSO}_3^-)$].^[36] The carboxylate stretches at 1567 cm^{-1} [$\nu_{\text{as}}(\text{CO})$] and 1402 cm^{-1} [$\nu_{\text{s}}(\text{CO})$] resemble those of the parent complex **7b**, which suggests that the *meta*-methoxybenzoate moiety in **7d** is also present in the $\mu_{1,3}$ -bridging mode. The IR spectrum of the dizinc complex **8d** compares well with that of **7d**, which shows distinct bands for the bridging *meta*-methoxybenzoate (1567 and 1402 cm^{-1}) and sulfonate groups (1238 cm^{-1}). The IR data of **7d** and **8d** are similar to the sulfonate complexes **7c** and **8c** coligated by 3-chlorobenzoate and acetate groups.^[21] Again a dependence of the IR absorptions of the coligands on the choice of the supporting ligand is not significant.

UV/Vis Spectroscopy

Electronic absorption spectra for the paramagnetic nickel complexes^[37] were registered in acetonitrile in the $300\text{--}1600 \text{ nm}$ range. The UV/Vis spectra of the chlorido-bridged nickel(II) complexes **1a** and **1b** are very similar, which is indicative of analogous face-sharing bioctahedral structures

for these complexes. The chlorido complex **1b** shows two weak absorption bands at 662 and 1007 nm that can be assigned to the spin-allowed ${}^3\text{A}_{2g} \rightarrow {}^3\text{T}_{1g}(\nu_2)$ and ${}^3\text{A}_{2g} \rightarrow {}^3\text{T}_{2g}(\nu_1)$ transitions of a nickel(II) ($S = 1$) ion.^[38] There is also a weak shoulder around 920 nm attributable to a spin-forbidden ${}^3\text{A}_{2g} \rightarrow {}^1\text{E}_g(\text{D})$ transition that is indicative of a significant distortion from octahedral symmetry.

Upon going from the chlorido complex **1b** to the carboxylato complexes **3b**, **5b**, and **7b**, the coordination environment of the Ni^{II} ions changes from $\text{N}_3\text{S}_2\text{Cl}$ to $\text{N}_3\text{S}_2\text{O}$. Therefore, a shift of the ν_1 transition – which is related to the octahedral splitting parameter Δ_o ($\Delta_o [\text{cm}^{-1}] = 10^7/\nu_1 [\text{nm}]$)^[34] – can be expected. This is indeed the case. The ν_1 transitions are redshifted by about $110\text{--}120 \text{ nm}$ relative to **1b**. The ν_1 and ν_2 values of the three pairs of analogous $[\text{Ni}_2\text{L}^1(\text{O}_2\text{CR})]^+$ and $[\text{Ni}_2\text{L}^2(\text{O}_2\text{CR})]^+$ complexes are not markedly different from one another. A dependence of the energy of these transitions on the substituent in the 4-position of the thiophenolate ligand is not significant.

The electronic absorption spectrum of the pale green sulfonato complex **7d** lacks the intense thiolate-to- Ni^{II} charge-transfer (CT) transitions seen in **7b**. This is in agreement with its formulation. The lack of the CT transitions in **7d** on the other hand, should facilitate an observation of the spin-allowed ${}^3\text{A}_{2g}(\text{F}) \rightarrow {}^3\text{T}_{1g}(\text{P})(\nu_3)$ transition [typical for Ni^{II} ($S = 1$) ions] in an octahedral coordination environment]. Indeed, there is a weak absorption at 400 nm that can be attributed to this d–d transition. Values of 400 nm for the ν_3 transition are typical for octahedral $\text{Ni}^{\text{II}}\text{N}_3\text{O}_3$ chromophores.^[21]

NMR Spectroscopy

To determine the solution structures, the zinc complexes were subjected to ${}^1\text{H}$ and ${}^{13}\text{C}$ NMR spectroscopic studies.

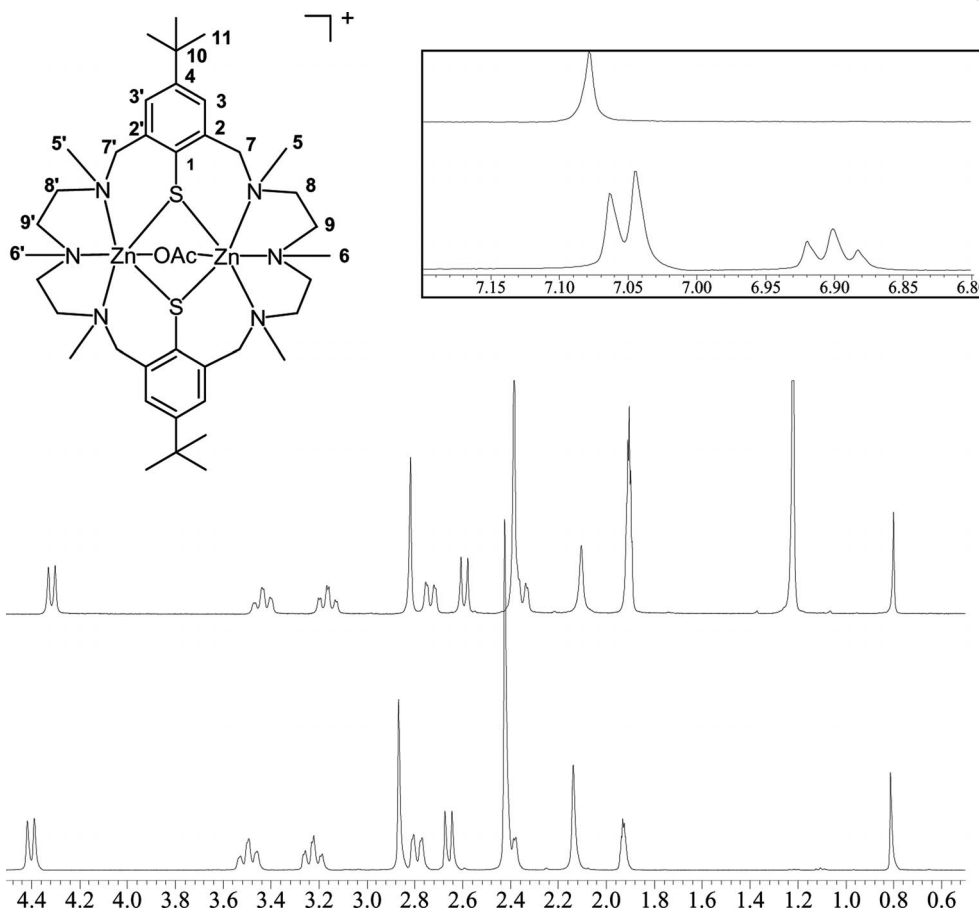


Figure 4. ^1H NMR spectra of **2a** (top) and **2b** (bottom) in CD_3CN at 295 K (4.5–0.6 ppm). The box shows the ^1H NMR spectra in the 7.15–6.80 ppm regions. The resonances for the complexes are listed in Table 2 and Table 3.

The ^1H and ^{13}C NMR spectra were recorded for sample solutions in CD_3CN at ambient temperature. Figure 4 shows the ^1H NMR spectrum of the acetato-bridged complex **2b**, which is representative of all the diamagnetic zinc thiophenolate complexes **4b**, **6b**, and **8b**. The ^1H NMR spectrum of **2a** is displayed for comparative purposes. Tables 2 and 3 list the ^1H and ^{13}C NMR spectroscopic data. The NMR spectroscopic data for **2a**, **4a**, **6a**, and **8a** are included for comparative purposes.

The ^1H NMR spectrum of complex **2b** displays one signal set indicative of the presence of a single isomer in solution. The six *N*-methyl groups give rise to two singlets ($4 \times \text{C}^5\text{H}_3$, $2 \times \text{C}^6\text{H}_3$), a clear indication for a C_{2v} -symmetric (type B, Figure 3) structure of the $[\text{Zn}_2\text{L}^2(\text{OAc})]^+$ cation. The ^{13}C NMR spectrum is also in agreement with structure B in that it reveals only 9 signals for the 30 carbon atoms of the $[\text{Zn}_2\text{L}^2]^+$ fragment. The methyl protons of the acetate group are observed at $\delta = 0.82$ ppm, significantly high-field shifted ($\Delta\delta = -1.01$ ppm) relative to free NaOAc ($\delta = 1.83$ ppm). A similar high-field shift was observed for **2a**.^[25] The high-field shift is attributable to the fact that the CH_3 protons of the acetate group are located above the center of the two phenyl rings of H_2L^2 in the shielding region.^[21]

The ^1H and ^{13}C NMR spectroscopic data of zinc complexes **4b** and **8b** are also in accord with a C_{2v} -symmetric structure (type B). Note, however, that **6b** reveals only 15 ^{13}C NMR spectroscopic signals and thus only half as many signals as expected for a C_1 -symmetric species (C_1 symmetry imparted on the complex by the asymmetric coligand, which has two stereo centers). The observation of the 15 signals implies a fast rotation of the carboxylate residue about the $\text{O}_2\text{C}-\text{R}$ bond, which leads to a time-averaged C_2 -symmetric structure on the NMR spectroscopy time-scale. A time-averaged C_2 symmetry is also evident in the ^1H NMR spectrum, particularly because the four CH_3 groups on the benzylic nitrogen atoms give rise to just two signals (instead of four for a species with a nonrotating carboxylate residue). A similar behavior was reported for the parent zinc complex **6a**.^[16]

The ^1H NMR spectrum of the sulfonate complex **8d** differs significantly from that of its parent complex **8b**. Particularly affected are the chemical shifts of the aromatic protons of this complex (Figure 5). A clear shift pattern is detectable. Thus, upon oxygenation the aromatic protons of the supporting ligand (C^3H and C^4H) are all low-field shifted, whereas the ones of the coligand are all shifted to higher field.

Table 2. Selected ^1H NMR spectroscopic data for zinc complexes **2a–8d**.^[a,b]

^1H NMR resonances of the coligand

	2b ^[16] [2a] ^[25,39]	4b [4a] ^[16]	6b [6a] ^[16]	8b	8d
	0.82 s [0.85] (CH ₃)	5.58 d [5.55 d] (C ² H)	1.05 m [0.93 m] C ^{2,5} H ₂	3.63 (s, C ⁸ H ₃)	3.69 (s, C ⁸ H ₃)
		6.77 d [6.74 d] (C ³ H)	1.10 m [1.10 m] C ^{2,5} H ₂	6.82 (m, C ⁷ H)	6.42 (s, C ³ H)
		7.25 m [7.23 m] ArH	1.28 s [1.30 s] C ⁸ H ₃	6.87 (s, C ³ H)	6.52 (m, C ⁷ H)
			1.43 s [1.41 s] C ⁹ H ₃	6.94 (m, C ⁶ H)	6.85 (m, C ⁶ H)
			1.51 m [1.45 m] C ^{2,5} H ₂	7.03 (t, C ⁵ H)	7.01 (t, C ⁵ H)
			3.05 m [3.05 m] C ¹ H		
			3.48 m [3.44 m] C ⁶ H		
			7.10 m [7.10 m, ArH]		

^1H NMR resonances of the [Zn₂L]²⁺ fragment^[a]

	2b ^[16] [2a] ^[25,40]	4b [4a] ^[16]	6b [6a] ^[16]	8b	8d
C ³ H	7.07 d [7.13 s]	7.01 d [7.03 s]	7.05 [7.12 s]	6.94 d	6.92 t
C ⁶ H	6.91 t [–]	6.76 t [–]	6.87 d [6.86 d]	6.65 t	7.07 d
C ⁵ H ₃	2.42 s [2.48 s]	2.53 s [2.53 s]	2.47 s [2.45 s]	2.55 s	2.50 s
			2.55 s [2.53 s]		
C ⁶ H ₃	2.89 s [2.92 s]	2.90 s [2.91 s]	2.88 s [2.88 s]	2.93 s	2.73 s
C ⁷ H ₂	2.68 d [2.62 d]	2.68 d [2.65 d]	2.67 m [2.68 d]	2.68 d	2.99 d
	4.40 d [4.40 d]	4.44 d [4.44 d]	4.42 d [4.41 d]	4.46 d	4.61 d
C ^{8,9} H ₂	2.38 m [2.40 m]	2.44 m [2.43 m]	2.43 m [2.43 m]	2.45 m	2.86-2.91
	2.78 m [2.83 m]	2.83 m [2.81 m]	2.80 m [2.79 m]	2.85 m	2.86-2.91
	3.21 m [3.29 m]	3.29 m [3.28 m]	3.26 m [3.23 m]	3.32 m	2.86-2.91
	3.48 m [3.52 m]	3.54 m [3.54 m]	3.53 m [3.52 m]	3.56 m	2.86-2.91
C ¹¹ H ₃	– [1.28 s]	– [1.06 s]	– [1.17 s]		–

[a] The data refer to the perchlorate salts. Resonances for the supporting ligands are assigned according to the structure shown in Figure 4. [b] Solvent: CD₃CN.

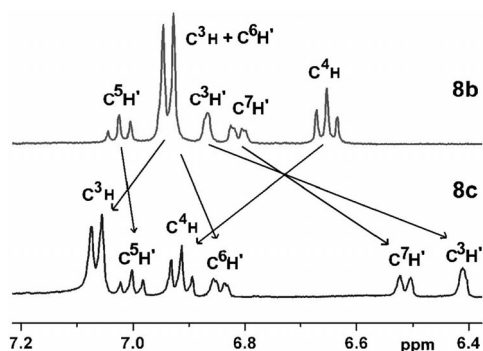


Figure 5. ^1H NMR resonances in the aromatic region (7.2–6.4 ppm) of the ^1H NMR spectra of complexes **8b** (top) and **8d** (bottom). The arrows indicate the up-field and down-field shifts of the resonances of the supporting ligand (C³H, C⁴H) and coligand (C⁵H', C⁶H', C⁷H', C³H').

The shift pattern noted above is not just a result of the conversion of the thiophenolate to sulfonate groups. The structural changes – that is the more pronounced folding of the phenyl rings of the supporting ligand in the sulfonate

complexes – also has to be taken into account. As is shown below, the *S*-oxygenation leads to a drastic decrease of the folding angle between the two aryl residues of the supporting ligand by approximately 45°. This in turn leads to much shorter distances between the coligand and the aryl rings of the macrocycle, such that the coligand senses a larger ring current. One would expect that this effect is larger for the *ortho* protons C³H' and C⁷H' (as they are closer to the aryl rings of H₂L⁴) in the coligands. This is indeed the case. The C³H' and C⁷H' signals are shifted by approximately 0.4 ppm. This value should be compared with much smaller shifts of only 0.10 and 0.02 ppm for the C⁶H' (*meta*) and C⁵H' (*para*) signals, respectively.

Description of the Crystal Structures

Single crystals of X-ray quality were obtained for the perchlorate salt of complex **5b** and the tetraphenylborate salt of complex **7d**. Ball-and-stick models of the structures of the two complexes are provided in Figures 6 and 8, respectively. Table 4 lists selected bond lengths and angles.

Table 3. Selected ^{13}C NMR spectroscopic data for zinc complexes **2a–8d**.^[a,b]

	2b ^[16] [2a]	4b [4a] ^[16]	6b [6a] ^[16]	8b	8d
[Zn ₂ L ²⁺] ²⁺ or [Zn ₂ L ¹⁺] ²⁺ fragment					
C ¹	147.8 [143.62]	147.16 [143.2]	147.5 [143.7]	147.40	145.07
C ²	136.2 [135.25]	136.24 [134.9]	135.7, 135.9 [135.3, 135.7]	135.57	133.87
C ³	132.3 [128.95]	131.82 [128.7]	131.7, 132.0 [128.8, 128.9]	131.76	132.17
C ⁴	123.2 [145.98]	122.78 [145.8]	123.1 [146.1]	122.79	127.76
C ⁵	47.2 [46.84]	46.94 [46.9]	47.2, 46.9 [46.6, 47.1]	47.11	43.78
C ⁶	50.2 [50.08]	49.79 [49.8]	49.9 [49.9]	49.84	44.00
C ⁷	58.4 [58.59]	58.36 [58.4]	57.9, 58.7 [58.0, 58.6]	58.42	51.51
C ⁸	60.0 [59.74]	59.61 [59.6]	59.4, 60.0 [59.5, 60.1]	59.73	56.11
C ⁹	64.7 [64.59]	64.32 [64.4]	64.1, 64.5 [64.6, 64.9]	64.31	62.86
C ¹⁰	– [34.64]	– [34.3]	– [34.5]	–	–
C ¹¹	– [31.68]	– [31.4]	– [31.6]	–	–
Coligand					
C1	175.5 [174.97]	169.71 [169.6]	39.5 [40.0]	168.97	166.28
C2	19.1 [22.94]	125.27 [125.2]	28.9 [29.5]	137.83	134.38
C3	–	128.16 [128.1]	124.3 [123.8]	114.47	113.28
C4	–	129.63 [129.5]	125.3 [126.0]	160.40	158.02
C5	–	130.04 [129.8]	32.0 [31.5]	117.54	117.46
C6	–	140.22 [139.9]	48.1 [48.1]	129.74	129.40
C7	–	obs. ^[c] [118.3]	177.6 [178.0]	122.01	122.12
C8	–	–	18.9 [19.0]	55.63	54.59
C9	–	–	19.0 [19.4]	–	–
C10	–	–	147.0 [146.5]	–	–
C11	–	–	126.5 [126.5]	–	–
C12	–	–	127.7 [127.8]	–	–
C13	–	–	129.0 [129.3]	–	–

[a] The data refer to the perchlorate salts. Resonances for the coligands and supporting ligands are assigned according to the structures shown in Figure 4 and Table 2. [b] Solvent: CD₃CN. [c] obsc. = obscured signal.

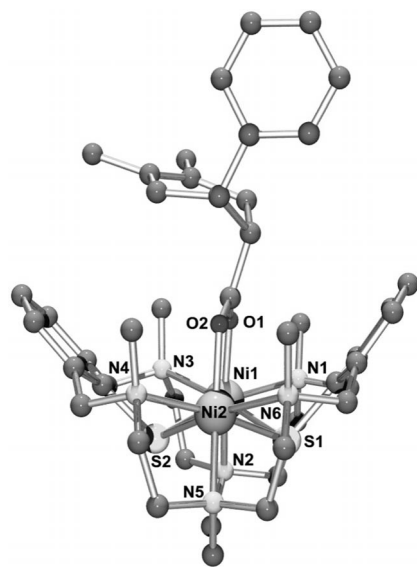


Figure 6. Molecular structure of the [Ni₂L²(μ-3,4-dimethyl-6-phenylcyclohex-3-enecarboxylate)]⁺ cation in crystals of **5b**[ClO₄] \cdot MeCN. Hydrogen atoms are omitted for clarity.

Table 4. Selected bond lengths [\AA] and angles [$^\circ$] in complexes **5a**,^[16] **5b**, **7c**,^[21] and **7d**.

	5a ^[16]	5b	7c ^[21]	7d
Ni1–O1/O7	2.043(2)	1.999(2)	2.040(5)	1.986(3)
Ni1–N1	2.285(2)	2.345(2)	2.230(7)	2.263(4)
Ni1–N2	2.173(2)	2.141(2)	2.136(6)	2.129(4)
Ni1–N3	2.223(2)	2.204(2)	2.265(6)	2.231(4)
Ni1–S1/O1	2.480(1)	2.479(1)	2.111(5)	2.048(3)
Ni1–S2/O5	2.4487(8)	2.456(1)	2.073(5)	2.098(3)
Ni2–O2/O8	1.994(2)	2.016(2)	2.009(5)	2.004(3)
Ni2–N4	2.265(2)	2.238(2)	2.266(6)	2.268(4)
Ni2–N5	2.159(2)	2.155(2)	2.131(7)	2.119(3)
Ni2–N6	2.293(2)	2.288(2)	2.254(7)	2.215(3)
Ni2–S1/O2	2.4982(7)	2.493(1)	2.102(5)	2.106(3)
Ni2–S2/O4	2.4256(9)	2.442(2)	2.109(5)	2.075(3)
Ni–N ^[a]	2.233(2)	2.229(2)	2.214(7)	2.204(4)
Ni–O(carboxylate) ^[a]	2.019(2)	2.008(2)	2.024(5)	1.995(3)
Ni–S/O(sulfonate) ^[a]	2.463(1)	2.468(1)	2.099(5)	2.082(3)
C–S ^[a]	1.763(2)	1.765(2)	1.783(8)	1.784(3)
Ni \cdots Ni	3.487(1)	3.473(1)	4.584(2)	4.535(1)
O1/O7–C39–O2/O8	126.88(18)	126.9(2)	129.4(7)	126.9(4)
Ni1–S1–Ni2	88.92(3)	88.62(4)	–	–
Ni1–S2–Ni2	91.33(2)	90.35(4)	–	–
Ph/Ph ^[b]	86.5	80.0	44.5	44.2

[a] Average values. [b] Folding angle between the normals of the planes of the two phenyl rings of the supporting ligand.

Selected crystallographic data are given in Table 6; see the CIF files for complete listings. The metrical parameters of complexes **5a**^[16] and [Ni₂L³(O₂CC₆H₄-3-Cl)]⁺,^[21] in which (L³)²⁻ represents the amine-sulfonate derivative of (L¹)²⁻, have been included for comparative purposes. A common labeling scheme for the core structures of analogous complexes was applied to facilitate structural comparisons.

Description of the Crystal Structure of **5b**[ClO₄] \cdot MeCN

This salt crystallizes in the triclinic space group $P\bar{1}$. The structure consists of well-separated [Ni₂L²(μ-3,4-dimethyl-6-phenylcyclohex-3-enecarboxylate)]⁺ cations, ClO₄⁻ anions, and MeCN solvate molecules. There are no unusual features as far as bond lengths and angles around the divalent Ni atoms are concerned. The average Ni–N, Ni–S, and Ni–O distances are 2.229(2), 2.468(1), and 2.008(2) Å, respectively. Similar values were observed in the parent complex **5a** [Ni–N 2.233(2) Å; Ni–S 2.463(1) Å; Ni–O 2.019(2) Å]^[16] and other carboxylato-bridged Ni₂ complexes of (L¹)²⁻.^[28,29,41] The mean C–S bond lengths in **5a** and **5b** are identical within experimental error. These C–S bonds are not affected upon conversion of the *t*Bu substituent to a H substituent.

It is worth noting that the phenyl and carboxylate groups of the coligand in **5b** assume bis-axial (ax,ax) positions, a conformation that is also seen for the parent complex **5a**.^[16] Generally, adjacent cyclohexene-ring substituents assume a more stable bis-equatorial (eq,eq) conformation (Figure 7).^[42,43] The presence of the ax,ax conformation is attributable to confinement, for example, to the form- (and size-) selective binding constraints of the cleftlike [Ni₂L²]²⁺ structure. A coordination of the cyclohexenecarboxylate in the alternative eq,eq conformation would inevitably lead to

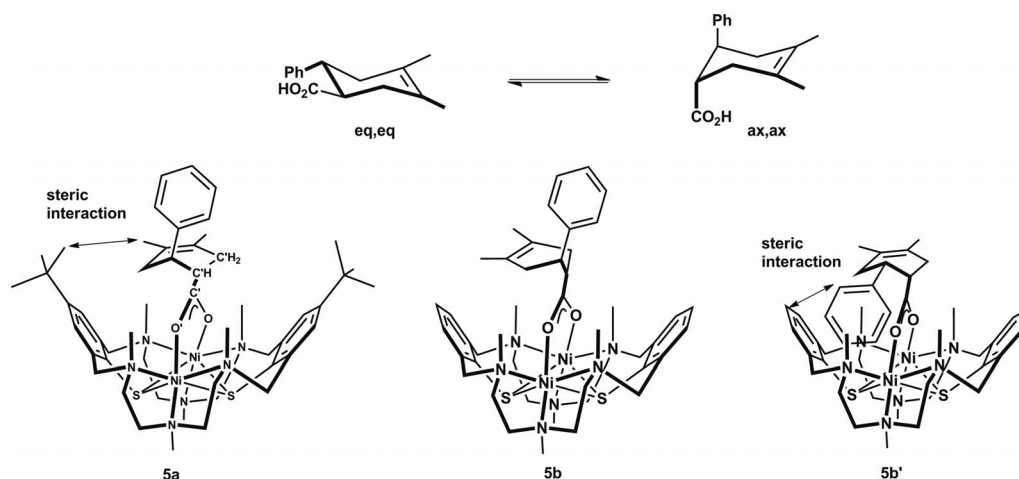


Figure 7. Top: The two possible eq,eq and ax,ax conformations of 3,4-dimethyl-6-phenylcyclohex-3-enecarboxylic acid. Bottom: Representation of the solid-state structures of **5a** and **5b** with the 3,4-dimethyl-6-phenylcyclohex-3-enecarboxylate coligand in the ax,ax conformation, and the structure of the hypothetical complex **5b'** with the cyclohexenecarboxylate in an alternative eq,eq conformation. Steric interactions between supporting ligands and coligands are indicated by double arrows. The primed C and O atoms in structure **5a** define the dihedral angle τ that is used in the text.

repulsive interactions between the phenyl rings of the coligand and the backbone of the supporting ligand as indicated in Figure 7 for a hypothetical structure of **5b'**. This stabilization of unusual ligand conformations by confinement is of general interest in supramolecular coordination chemistry.^[44]

The only other significant structural differences between complexes **5a** and **5b** concern a smaller twist angle of the carboxylate substituent with respect to the cyclohexene ring in **5b** (expressed by the dihedral angle τ , see legend to Figure 7); and a smaller folding angle between the planes through the two aryl rings of the supporting ligand in **5b**. The smaller τ value in **5b** of 163.5° (O2–C31–C32–C33) as opposed to 174.8° (O2–C39–C40–C45) in **5a** can be attributed to the absence of repulsive interactions between the *t*Bu groups of the supporting ligand and CH₃ groups of the coligand (indicated by the hypothetical structure of **5b'** in Figure 7). The same arguments can be invoked to explain the decrease of the folding angle between the two aryl rings from 86.5° in **5a** to 80.0° in **5b**.

Description of the Crystal Structure of $7d[\text{BPh}_4] \cdot 0.5\text{MeCN} \cdot 0.5\text{H}_2\text{O}$

The crystal structure of $7d[\text{BPh}_4] \cdot 0.5\text{MeCN} \cdot 0.5\text{H}_2\text{O}$ confirms the formulation of **7d** as a dinuclear nickel(II) complex supported by the deprotonated macrocyclic amine-sulfonate ligand (L^4)²⁻. The crystal structure consists of discrete $[\text{Ni}_2\text{L}^4(\text{O}_2\text{CC}_6\text{H}_4\text{-3-OMe})]^+$ cations, BPh_4^- anions, MeCN, and H₂O solvate molecules. Figure 8 provides a ball-and-stick model of the structure of cation **7d**. Table 4 lists selected bond lengths and angles. The carboxylate and both sulfonate groups bridge the divalent Ni ions in a $\mu_{1,3}$ fashion at a Ni...Ni distance of $4.535(1)$ Å, a distance approximately one Å larger than in the thiophenolate complexes. The amine nitrogen atoms of (L^4)²⁻ occupy the remaining positions and complete the pseudo-octahedral Ni_3O_3 coordination spheres. The mean Ni–O^{carboxylate} bond

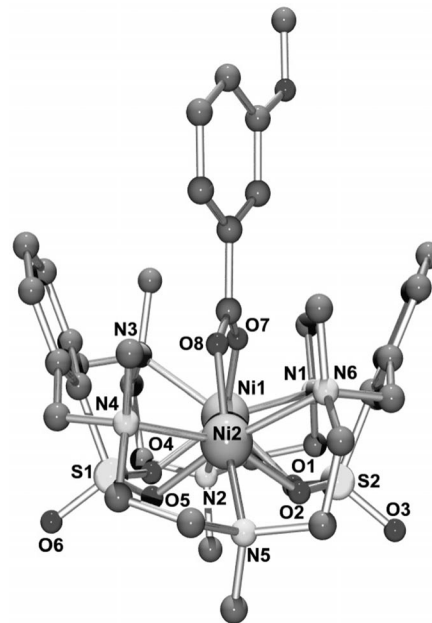


Figure 8. Molecular structure of the $[\text{Ni}_2\text{L}^4(\mu\text{-O}_2\text{CC}_6\text{H}_4\text{OMe})]^+$ cation (ball-and-stick model) in crystals of $7d[\text{BPh}_4] \cdot 0.5\text{MeCN} \cdot 0.5\text{H}_2\text{O}$. Hydrogen atoms are omitted for clarity.

is of length $1.995(3)$ Å and significantly shorter than the average Ni–O^{sulfonate} bonding length of $2.082(3)$ Å, thereby indicating stronger Ni–O^{carboxylate} bonds. This is not surprising given that carboxylate ligands are generally much better donor ligands than sulfonate ligands.^[45] The mean Ni–N and Ni–O distances at $2.204(2)$ and $2.053(3)$ Å, respectively, resemble those in the amine-sulfonate complex $[\text{Ni}_2\text{L}^3(\text{O}_2\text{CC}_6\text{H}_4\text{-3-Cl})]^+$ (**7e**), in which (L^3)²⁻ represents the amine-sulfonate derivative of (L^1)²⁻ [$2.214(7)$, $2.074(5)$ Å].^[21]

Of note is a very acute angle of 44.2° at which the best planes through the two phenyl rings of the amine-sulfonate

macrocycle intersect. A similar value of 44.5° is observed in **7c**, the only other example of a Ni_2 complex of a Robson-type amino-sulfonate complex that has been characterized crystallographically so far.^[21] The two complexes are essentially isostructural and the corresponding bond lengths and angles lie within very narrow ranges. Based on the NMR spectroscopic data, a similar decrease of the folding angle is likely for the zinc complex **8d**.

Complex Stability

We decided to determine the relative stability constants of some analogous zinc complexes supported by H_2L^1 and H_2L^2 to probe whether the presence or absence of the two *tert*-butyl substituents affects the thermodynamic stability of the complexes. For this purpose the relative stability constants (K_{rel}) of the formiato-, acetato-, palmitato-, chloroacetato-, and benzoato-bridged zinc complexes **2a**, **2b**, and **9a–12b** were determined by the exchange experiments in Equation (1).



		$n = 1$	$n = 2$
2a ($n = 1$)	R = H	9a	9b
2b ($n = 2$)	R = $\text{C}_{15}\text{H}_{31}$	10a	10b
	R = CH_2Cl_2	11a	11b
	R = Ph	12a	12b

The reactions were performed in a 1:1 molar ratio, and the equilibria are attained within sample preparation. The relative concentrations of the complexes were determined by integration of the ^1H NMR spectroscopic signals for the methyl protons for the free acetate ion ($\delta = 1.83$ ppm) and the acetato ligand of complexes **2a** ($\delta = 0.85$ ppm) or **2b** ($\delta = 0.86$ ppm), respectively. The relative stability constants were then calculated with the mass action law in Equation (2).

$$K_{\text{rel}} = \frac{[\mathbf{9a,b-12a,b}][\text{NaOAc}]}{[\mathbf{2a,b}][\text{RCO}_2\text{Na}]} \quad (2)$$

Table 5 lists the stability constants (relative to **2a** or **2b**) and the $\text{p}K_{\text{a}}$ values of the corresponding carboxylic acids.^[46] As can be seen, the equilibrium constants differ by as much as two orders of magnitude and do not correlate with the $\text{p}K_{\text{a}}$ values of the carboxylates. The complex stability constants can be ranked as follows **9a** < **2a** < **11a** < **10a** < **12a** for the $[\text{Zn}_2\text{L}^1(\text{O}_2\text{CR})]^{+}$ complexes and **9b** < **11b** < **2b** < **10b** < **12b** for the $[\text{Zn}_2\text{L}^2(\text{O}_2\text{CR})]^{+}$ complexes. For both series, a clear trend is seen. Thus, the larger the organic residue R of the carboxylate anion (RCO_2^-) the larger

Table 5. Relative stability constants of the zinc complexes **2a**, **2b**, and **9a–12b**.

Coligand	$\text{p}K_{\text{a}}$	K_{rel} (2a)	$\Delta\Delta G^{\text{[a]}}$ [kJ mol $^{-1}$]	K_{rel} (2b)	$\Delta\Delta G^{\text{[a]}}$ [kJ mol $^{-1}$]
9a,b	HCO_2^-	3.75	−5.71	0.20	−4.00
10a,b	$\text{C}_{15}\text{H}_{31}\text{CO}_2^-$	5.70	5.00	3.30	2.96
11a,b	$\text{CH}_2\text{ClCO}_2^-$	2.82	0.24	0.30	−2.98
12a,b	PhCO_2^-	4.20	5.53	3.75	3.28

[a] $K_{\text{rel}} = \exp(\Delta\Delta G/RT)$.

the binding constant, the maximum value being reached for the benzoato-bridged complexes. However, the stability differences are much less pronounced in the complexes of the de-*tert*-butylated macrocycle (L^2) $^{2-}$. This observation can be traced back to the less extensive $\text{CH}\cdots\pi$ or van der Waals interactions in the $[\text{Zn}_2\text{L}^2(\text{O}_2\text{CR})]^{+}$ complexes. In contrast to **7d**, for example, complex **7c** reveals short distances (3.23 and 3.31 Å) between the coligand and the *tert*-butyl protons of the supporting macrocycle.

Conclusion

In summary, a series of novel nickel(II) and zinc(II) complexes supported by macrocyclic amine thiophenolate and amine phenylsulfonate ligands have been synthesized and characterized, namely, $[\text{Ni}^{\text{II}}_2\text{L}^2(\text{Cl})]^{+}$ (**1b**), $[\text{Zn}^{\text{II}}_2\text{L}^2(\text{OAc})]^{+}$ (**2b**), $[\text{Ni}^{\text{II}}_2\text{L}^2(\text{O}_2\text{CCH}=\text{CHPh})]^{+}$ (**3b**), $[\text{Zn}^{\text{II}}_2\text{L}^2(\text{O}_2\text{CCH}=\text{CHPh})]^{+}$ (**4b**), $[\text{Ni}^{\text{II}}_2\text{L}^2(\text{O}_2\text{CC}_{14}\text{H}_{17})]^{+}$ (**5b**), $[\text{Zn}^{\text{II}}_2\text{L}^2(\text{O}_2\text{CC}_{14}\text{H}_{17})]^{+}$ (**6b**, in which $\text{C}_{14}\text{H}_{17}\text{CO}_2^- = 3,4$ -dimethyl-6-phenylcyclohex-3-enecarboxylate), $[\text{Ni}^{\text{II}}_2\text{L}^2(\text{O}_2\text{CC}_6\text{H}_4\text{-3-OMe})]^{+}$ (**7b**), $[\text{Zn}^{\text{II}}_2\text{L}^2(\text{O}_2\text{CC}_6\text{H}_4\text{-3-OMe})]^{+}$ (**8b**), $[\text{Ni}^{\text{II}}_2\text{L}^4(\text{O}_2\text{CC}_6\text{H}_4\text{-3-OMe})]^{+}$ (**7d**), and $[\text{Zn}^{\text{II}}_2\text{L}^4(\text{O}_2\text{CC}_6\text{H}_4\text{-3-OMe})]^{+}$ (**8d**). The de-*tert*-butylated macrocycles H_2L^2 and H_2L^4 behave essentially in the same fashion as H_2L^1 (and H_2L^3) by producing dinuclear mixed-ligand $[\text{M}_2\text{L}^2(\mu\text{-L}')^{+}]$ complexes with analogous calixarene-like structures as shown by X ray crystallography and NMR spectroscopy. The major difference between the $[\text{M}_2\text{L}^1(\mu\text{-L}')^{+}]$ and $[\text{M}_2\text{L}^2(\mu\text{-L}')^{+}]$ complexes concerns the size of the binding pocket of the compounds, which is greatly reduced upon going from H_2L^1 to H_2L^2 . This causes significant structural differences between complexes **5a** and **5b**, for instance, through a smaller twist angle of the carboxylate substituent with respect to the cyclohexene ring in **5b**, and a smaller folding angle between the planes through the two aryl rings of the supporting ligand in **5b**. The smaller τ value in **5b** of 163.5° ($\text{O}2\text{-C}31\text{-C}32\text{-C}33$) as opposed to 174.8° ($\text{O}2\text{-C}39\text{-C}40\text{-C}45$) in **5a** can be attributed to the absence of repulsive interactions between the *tert*-butyl groups of the supporting ligand and CH_3 groups of the coligand. Another significant difference associated with removal of the *tert*-butyl substituents concerns the less pronounced differences of the relative stability constants for the carboxylato-bridged $[\text{M}_2\text{L}^2(\mu\text{-O}_2\text{CR})]^{+}$ complexes {as compared to the $[\text{M}_2\text{L}^1(\mu\text{-O}_2\text{CR})]^{+}$ complexes}. These stability differences can be explained in terms of less pronounced intramolecular $\text{CH}\cdots\pi$ and/or van der Waals interactions in the de-*tert*-butylated complex systems.

Experimental Section

General: Unless otherwise noted the preparations were carried out under an argon atmosphere by using standard Schlenk techniques. The ligand H_2L^2 ^[24] and 3,4-dimethyl-6-phenylcyclohex-3-enecarboxylic acid^[47] were prepared as described in the literature. Melting points were determined in capillaries. The infrared spectra were recorded as KBr discs using a Bruker VECTOR 22 FTIR spectro-

photometer. Electronic absorption spectra were recorded on a Jasco V-570 UV/Vis/near-IR spectrophotometer. ESI-FTICR mass spectra were recorded with a Bruker-Daltonics Apex II instrument using dilute $\text{CH}_2\text{Cl}_2/\text{MeOH}$ solutions. NMR spectra were recorded on a Bruker AVANCE DPX-200, a Varian Unity 300, or Bruker 400 and 500 spectrometers at 295 K. Chemical shifts refer to solvent signals.

Caution! Perchlorate salts of transition-metal complexes are hazardous and may explode. Only small quantities should be prepared and handled with great care.

[Ni₂L²(μ-Cl)]ClO₄ (1b[ClO₄]): A solution of $\text{NiCl}_2 \cdot 6\text{H}_2\text{O}$ (183 mg, 0.77 mmol) in methanol (5 mL) was added to a solution of $\text{H}_2\text{L}^2 \cdot 6\text{HCl}$ (0.300 g, 0.385 mmol) in methanol (20 mL) followed by triethylamine (0.311 g, 3.08 mmol). After stirring for 2 d at room temperature, solid $\text{LiClO}_4 \cdot 3\text{H}_2\text{O}$ (1.00 g, 6.23 mmol) was added. The yellow solid was filtered and washed with diethyl ether. An analytical sample was obtained by recrystallization from acetonitrile; yield 0.221 g (71%); m.p. 341–342 °C (dec.). $\text{C}_{30}\text{H}_{48}\text{Cl}_2\text{N}_6\text{Ni}_2\text{O}_4\text{S}_2$ (809.16): calcd. C 44.53, H 5.98, N 10.39, S 7.93; found C 44.03, H 6.41, N 10.16, S 7.88. IR (KBr): $\tilde{\nu}$ = 3011 (m), 2967 (m), 2860 (s), 2811 (m), 1633 (w), 1486 (m), 1461 (s), 1418 (m), 1394 (w), 1368 (w), 1355 (w), 1342 (w), 1290 (w), 1260 (w), 1209 (w), 1198 (w), 1180 (w), 1095 (s) $\nu_3(\text{ClO}_4^-)$, 1030 (w), 957 (w), 932 (m), 921 (m), 897 (w), 832 (w), 822 (m), 795 (w), 773 (s), 753 (w), 735 (w), 671 (w), 651 (w), 623 (s) $\nu_4(\text{ClO}_4^-)$, 570 (w), 544 (w), 496 (w), 459 (w), 422 (w) cm^{-1} .

[Zn₂L²(μ-OAc)]ClO₄ (2b[ClO₄]): A solution of $\text{Zn}(\text{OAc})_2 \cdot 2\text{H}_2\text{O}$ (283 mg, 1.28 mmol) in methanol (5 mL) was added to a solution of $\text{H}_2\text{L}^2 \cdot 6\text{HCl}$ (500 mg, 0.643 mmol) in methanol (20 mL). A solution of triethylamine (520 mg, 5.14 mmol) in methanol (5 mL) was added and the resulting clear solution was stirred for 2 d at room temperature. Solid $\text{LiClO}_4 \cdot 3\text{H}_2\text{O}$ (1.00 g, 6.23 mmol) was then added. The resulting colorless precipitate was isolated by filtration, washed with methanol, and dried in air. The product was recrystallized from an acetonitrile/ethanol mixture; yield 468 mg, 0.550 mmol (86%); m.p. 320–321 °C. $\text{C}_{32}\text{H}_{51}\text{ClN}_6\text{O}_6\text{S}_2\text{Zn}_2 \cdot \text{H}_2\text{O}$ (846.15 + 18.02): calcd. C 44.48, H 6.18, N 9.73, S 7.42; found C 44.10, H 5.81, N 9.69, S 7.95. IR (KBr): $\tilde{\nu}$ = 2979 (s), 2993 (s), 2851 (s), 2805 (s), 1583 (s) [$\nu_{\text{as}}(\text{OAc})$], 1460 (s), 1433 (s) [$\nu_{\text{s}}(\text{OAc})$], 1395 (m), 1365 (m), 1350 (w), 1312 (w), 1295 (m), 1269 (m), 1203 (w), 1171 (m), 1095 (vs) [$\nu(\text{ClO}_4^-)$], 1042 (s), 1060 (s), 1003 (m), 959 (w), 915 (m), 894 (w), 824 (m), 749 (w), 728 (w), 663 (m), 622 (s), 561 (m), 533 (w), 523 (w), 482 (w), 411 (w) cm^{-1} . The tetraphenylborate salt, $[\text{Zn}_2\text{L}^2(\text{OAc})]\text{BPh}_4$ (2b[BPh₄]), was prepared by adding NaBPh_4 (342 mg, 1.00 mmol) to a solution of 2b[ClO₄] (85 mg, 0.100 mmol) in methanol (40 mL). The colorless microcrystalline solid was isolated by filtration, washed with ethanol, and dried in air.

[Ni₂L²(μ-O₂CCH=CHPh)]ClO₄ (3b[ClO₄]): A solution of triethylammonium cinnamate [prepared in situ from cinnamic acid (37 mg, 0.25 mmol) and triethylamine (25.3 mg, 0.25 mmol)] in methanol (5 mL) was added to a solution of 1b[ClO₄] (100 mg, 0.124 mmol) in methanol (20 mL). After stirring for 2 h at ambient temperature, the product was precipitated by the addition of solid $\text{LiClO}_4 \cdot 3\text{H}_2\text{O}$ (301 mg, 1.87 mmol). The green microcrystalline solid was isolated by filtration, washed with cold methanol (2 mL), and recrystallized once from a mixed ethanol/acetonitrile solvent system; yield 80 mg (70%); m.p. 318–319 °C (dec.). $\text{C}_{39}\text{H}_{55}\text{ClN}_6\text{Ni}_2\text{O}_6\text{S}_2 \cdot \text{H}_2\text{O}$ (920.86 + 18.02): calcd. C 49.89, H 6.12, N 8.95, S 6.83; found C 49.94, H 6.34, N 8.99, S 7.25. IR (KBr): $\tilde{\nu}$ = 2996 (m), 2966 (m), 2861 (s), 2811 (s), 1642 (m) [$\nu(\text{C}=\text{C})$], 1577 (s) [$\nu_{\text{as}}(\text{C}-\text{O})$], 1491 (m), 1461 (s), 1450 (s), 1435 (m), 1424 (s), 1406

(s) [$\nu_{\text{s}}(\text{RCO}_2^-)$], 1366 (w), 1351 (w), 1337 (w), 1298 (w), 1267 (w), 1202 (w), 1171 (w), 1092 (s), 1040 (s), 1003 (w), 965 (m), 921 (m), 894 (w), 868 (w), 828 (m), 806 (w), 765 (m), 726 (w), 708 (w), 687 (w), 670 (w), 622 (m), 599 (w), 564 (w), 537 (w), 524 (w), 485 (w), 436 (w), 415 (w) cm^{-1} .

[Zn₂L²(μ-O₂CCH=CHPh)]ClO₄ (4b[ClO₄]): A solution of triethylammonium cinnamate [prepared in situ from cinnamic acid (524 mg, 3.54 mmol) and triethylamine (179 mg, 1.77 mmol)] in methanol (5 mL) was added to a solution of 2b[ClO₄] (300 mg, 0.354 mmol) in methanol (50 mL). After stirring for 12 h at ambient temperature, the solvent was removed under reduced pressure to a final volume of approximately 10 mL. The colorless solid was isolated by filtration and washed with cold methanol (5 mL). To remove traces of unreacted starting compound 2b[ClO₄], the product was treated again with a tenfold molar excess amount of triethylammonium cinnamate as described above. Recrystallization from a mixed ethanol/acetonitrile solvent system gave the title compound in an analytically pure form; yield 240 mg (73%); m.p. 325–328 °C (dec.). $\text{C}_{39}\text{H}_{55}\text{ClN}_6\text{O}_6\text{S}_2\text{Zn}_2$ (934.25): calcd. C 50.14, H 5.93, N 9.00, S 6.86; found C 49.66, H 6.07, N 8.97, S 7.01. IR (KBr): $\tilde{\nu}$ = 2991 (m), 2860 (s), 1641 (m) [$\nu(\text{C}=\text{C})$], 1570 (s) [$\nu_{\text{as}}(\text{CO})$], 1485 (m), 1460 (s), 1433 (s), 1401 (s) [$\nu_{\text{s}}(\text{CO})$], 1367 (m), 1352 (w), 1333 (w), 1312 (w), 1296 (m), 1269 (m), 1204 (w), 1172 (w), 1093 (vs) [$\nu_3(\text{ClO}_4^-)$], 1043 (s), 1003 (m), 969 (m), 917 (m), 893 (w), 871 (w), 825 (s), 803 (w), 765 (s), 727 (w), 707 (w), 687 (w), 666 (w), 623 (s) [$\nu_4(\text{ClO}_4^-)$], 594 (w), 561 (w), 535 (w), 522 (w), 483 (w), 454 (w), 409 (w) cm^{-1} .

[Ni₂L²(μ-O₂CC₁₄H₁₇)]ClO₄ (5b[ClO₄]): A solution of triethylammonium 3,4-dimethyl-6-phenylcyclohex-3-enecarboxylate [prepared in situ from 3,4-dimethyl-6-phenylcyclohex-3-enecarboxylic acid (58 mg, 0.25 mmol) and triethylamine (25.3 mg, 0.25 mmol)] in methanol (5 mL) was added to a solution of 1b[ClO₄] (100 mg, 0.124 mmol) in methanol (50 mL). After stirring for 2 h at ambient temperature, the product was precipitated by the addition of solid $\text{LiClO}_4 \cdot 3\text{H}_2\text{O}$ (301 mg, 1.87 mmol). The green microcrystalline solid was isolated by filtration, washed with cold methanol (2 mL), and recrystallized once from a mixed ethanol/acetonitrile solvent system; yield 89 mg (72%); m.p. 289–290 °C (dec.). $\text{C}_{45}\text{H}_{65}\text{ClN}_6\text{Ni}_2\text{O}_6\text{S}_2$ (1003.00): calcd. C 53.89, H 6.53, N 8.38, S 6.39; found C 53.75, H 6.44, N 8.13, S 6.02. IR (KBr): $\tilde{\nu}$ = 2996 (m), 2856 (s), 1575 (s) [$\nu_{\text{as}}(\text{CO})$], 1488 (w), 1461 (s), 1425 (s), 1409 (m) [$\nu_{\text{s}}(\text{CO})$], 1309 (w), 1297 (w), 1266 (w), 1201 (w), 1172 (w), 1094 (s) [$\nu_3(\text{ClO}_4^-)$], 1041 (m), 1002 (m), 956 (w), 917 (m), 893 (w), 827 (m), 805 (w), 770 (m), 749 (w), 717 (w), 700 (w), 670 (w), 623 (s), 564 (w), 536 (w) cm^{-1} .

[Zn₂L²(μ-O₂CC₁₄H₁₇)]ClO₄ (6b[ClO₄]): A solution of triethylammonium 3,4-dimethyl-6-phenylcyclohex-3-enecarboxylate [prepared in situ from 3,4-dimethyl-6-phenylcyclohex-3-enecarboxylic acid (272 mg, 1.18 mmol) and triethylamine (119 mg, 1.18 mmol)] in methanol (5 mL) was added to a solution of 2b[ClO₄] (100 mg, 0.118 mmol) in methanol (20 mL). After stirring for 12 h at ambient temperature, the solvent was removed under reduced pressure to a final volume of approximately 10 mL. The colorless solid was isolated by filtration and washed with cold methanol (2–3 mL). To remove traces of unreacted starting compound 2b[ClO₄] the product was treated again with a tenfold molar excess amount of triethylammonium 3,4-dimethyl-1,6-phenylcyclohex-3-enecarboxylate as described above. Recrystallization from a mixed ethanol/acetonitrile solvent system gave the title compound in analytically pure form; yield 90 mg (75%); m.p. 275–276 °C (dec.). $\text{C}_{45}\text{H}_{65}\text{ClN}_6\text{O}_6\text{S}_2\text{Zn}_2$ (1016.40): calcd. C 53.18, H 6.45, N 8.27, S 6.31; found C 53.03, H 6.74, N 7.85, S 5.42. IR (KBr): $\tilde{\nu}$ = 3057

(w), 2292 (m), 2856 (s), 1573 (s) [$\nu_{\text{as}}(\text{CO})$], 1483 (m), 1460 (s), 1426 (s), 1408 (s) [$\nu_{\text{s}}(\text{CO})$], 1367 (w), 1352 (w), 1311 (m), 1295 (m), 1269 (m), 1202 (w), 1172 (w), 1095 (s) [$\nu_3(\text{ClO}_4)$], 1002 (w), 1005 (m), 957 (w), 925 (w), 915 (m), 893 (w), 843 (w), 825 (m), 802 (w), 771 (m), 728 (w), 716 (w), 700 (w), 666 (w), 623 (s) [$\nu_4(\text{ClO}_4)$], 580 (w), 560 (w), 536 (w), 523 (w) cm^{-1} .

[Ni₂L²(μ -O₂CC₆H₄-3-OMe)](ClO₄) (7b(ClO₄)): Triethylamine (37.5 mg, 0.37 mmol) was added to a solution of 3-methoxybenzoic acid (56.4 mg, 0.371 mmol) in methanol (5 mL). This solution was added to a solution of **1b**(ClO₄) (150 mg, 0.185 mmol) in methanol (20 mL). After stirring for 2 h, solid LiClO₄·3H₂O (300 mg, 1.95 mmol) was added. The green solid was filtered, washed with MeOH, and dried under vacuum. The crude product was purified by recrystallization from acetonitrile/ethanol; yield 148 mg (0.160 mmol, 86% based on **1b**); m.p. 337–338 °C (dec.). C₃₈H₅₅ClN₆Ni₂O₇S₂ (924.849): calcd. C 49.35, H 5.99, N 9.09, S 6.93; found C 49.64, H 5.88, N 9.21, S 7.22. IR (KBr): $\tilde{\nu}$ = 3517 (m), 2994 (m), 2967 (s), 2860 (s), 1598 (m) [$\nu(\text{CC})$],^[48] 1574 (s) [$\nu_{\text{as}}(\text{CO})$], 1487 (m), 1462 (s), 1426 (s), 1399 (s) [$\nu_{\text{s}}(\text{CO})$], 1363 (m), 1335 (w), 1312 (m), 1298 (m), 1279 (w), 1265 (w), 1254 (m), 1201 (w), 1170 (w), 1095 (vs) [$\nu_3(\text{ClO}_4^-)$], 1040 (s), 1000 (m), 957 (w), 918 (m), 894 (w), 866 (w), 828 (m), 806 (m), 788 (m), 763 (s), 726 (w), 691 (w), 670 (w), 623 (m) [$\nu_4(\text{ClO}_4^-)$], 565 (w), 537 (w), 526 (w), 492 (w), 461 (w), 440, (w), 416 (w) cm^{-1} .

[Zn₂L²(μ -O₂CC₆H₄-3-OMe)](ClO₄) (8b(ClO₄)): A solution of triethylammonium 3-methoxybenzoate [prepared in situ from 3-methoxybenzoic acid (269 mg, 1.77 mmol) and triethylamine (178 mg, 1.77 mmol)] in methanol (5 mL) was added to a solution of **2b**(ClO₄) (150 mg, 0.177 mmol) in methanol (20 mL). After stirring for 12 h at ambient temperature, the solvent was removed under reduced pressure to a final volume of approximately 10 mL. The colorless solid was isolated by filtration and washed with cold methanol (5 mL). To remove traces of unreacted starting compound **2b**(ClO₄), the product was treated again with a tenfold molar excess amount of triethylammonium 3-methoxybenzoate as described above. Recrystallization from a mixed ethanol/acetonitrile solvent system then gave the title compound in analytically pure form; yield 145 mg (87%); m.p. 345 °C (dec.). C₃₈H₅₅ClN₆O₇S₂Zn₂·H₂O (938.24 + 18.02): calcd. C 47.73, H 6.01, N 8.79, S 6.71; found C 47.31, H 5.61, N 8.47, S 7.21. IR (KBr): $\tilde{\nu}$ = 3525 (m), 2991 (m), 2857 (s), 1598 (m), 1570 (s) [$\nu_{\text{as}}(\text{CO})$], 1484 (m), 1462 (s), 1426 (s), 1399 (s) [$\nu_{\text{s}}(\text{CO})$], 1367 (m), 1352 (m), 1333 (m), 1313 (m), 1297 (m), 1280 (m), 1269 (m), 1251 (m), 1204 (w), 1172 (w), 1096 (vs) [$\nu_3(\text{ClO}_4^-)$], 1042 (s), 1003 (m), 959 (w), 916 (m), 894 (m), 868 (w), 825 (m), 803 (m), 784 (m), 764 (s), 727 (w), 688 (w), 666 (w), 623 (m) [$\nu_4(\text{ClO}_4^-)$], 562 (w), 536 (w), 523 (w), 483 (w), 433 (w), 410 (w) cm^{-1} .

[Ni₂L⁴(μ -O₂CC₆H₄-3-OMe)](ClO₄) (7d(ClO₄)): A solution of MCPBA (81 mg, 0.47 mmol) in acetonitrile (2 mL) was added dropwise at 0 °C to a solution of **7b**(ClO₄) (60 mg, 0.065 mmol) in acetonitrile (20 mL). After stirring for 10 min at room temperature, solid LiClO₄·3H₂O (500 mg, 3.26 mmol) was added followed by ethanol (20 mL). The product precipitated upon evaporation to a final volume of approximately 5 mL. The resulting lime-green solid was filtered and purified by recrystallization from acetonitrile/ethanol; yield 55 mg (0.054 mmol, 83%); m.p. 317–318 °C (dec.). IR (KBr): $\tilde{\nu}$ = 3555 (s), 3497 (m), 2992 (m), 2871 (s), 1603 (s) [$\nu(\text{CC})$], 1567 (s) [$\nu_{\text{as}}(\text{CO})$], 1461 (s), 1426 (s), 1399 (s) [$\nu_{\text{s}}(\text{CO})$], 1359 (w), 1312 (w), 1208 (s) [$\nu_{\text{s}}(\text{SO}_3)$], 1178 (s), 1134 (s), 1088 (vs) [$\nu_3(\text{ClO}_4^-)$], 1035 (s), 993 (w), 975 (w), 910 (m), 869 (w), 832 (m), 810 (w), 781 (s), 762 (s), 742 (w), 700 (s), 661 (w), 651 (w), 624 (s) [$\nu_4(\text{ClO}_4^-)$], 586 (w), 567 (m), 527 (w), 497 (w), 430 (w) cm^{-1} . Addition of NaBPh₄

(60.0 mg, 0.175 mmol) to a solution of **7d**(ClO₄) (60 mg, 0.059 mmol) in acetonitrile (20 mL) provides, after addition of ethanol (20 mL) and concentration to approximately 10 mL, pale green crystals of crude product, which can be purified by recrystallization from ethanol/acetonitrile; yield 50 mg (0.040 mmol, 68%); m.p. 298–299 °C. C₆₂H₇₅BN₆Ni₂O₉S₂ (1240.62): calcd. C 60.02, H 6.09, N 6.77, S 5.17; found C 59.85, H 5.74, N 6.88, S 5.27. IR (KBr): $\tilde{\nu}$ = 3494 (m), 3053 (m), 3032 (m), 2997 (m), 2868 (m), 1598 (m) [$\nu(\text{CC})$], 1569 (s) [$\nu_{\text{as}}(\text{CO})$], 1478 (s), 1426 (m), 1401 (s) [$\nu_{\text{s}}(\text{CO})$], 1357 (w), 1312 (w), 1240 (s), 1204 (s) [$\nu(\text{SO})$], 1174 (w), 1141 (m), 1087 (s), 1033 (s), 993 (w), 974 (w), 917 (w), 907 (w), 831 (w), 809 (w), 777 (m), 762 (m), 737 (s) [$\nu(\text{BPh}_4)$], 700 (s) [$\nu(\text{BPh}_4)$], 662 (w), 651 (w), 624 (s), 615, (w), 582 (w), 568 (w), 528 (w), 498 (w), 474 (w), 430 (w) cm^{-1} .

[Zn₂L³(μ -O₂CC₆H₄-3-OMe)](ClO₄) (8d(ClO₄)): Hydrogen peroxide (2.00 mL, 35 wt.-% solution in water, 20.6 mmol) was added to a solution of **8b**(ClO₄) (250 mg, 0.270 mmol) in methanol (50 mL). The reaction mixture was left at reflux for 5 h and was then filtered. After cooling to room temperature, the solution was concentrated to give the crude product as a white powder. Recrystallization from ethanol/acetonitrile provided pure **8d**(ClO₄) (105 mg, 38%); m.p. 358–359 °C. C₃₈H₅₅ClN₆O₁₃S₂Zn₂·H₂O (1034.22 + 18.02): calcd. C 43.37, H 5.46, N 7.99, S 6.09; found C 43.02, H 5.00, N 8.21, S 6.32. IR (KBr): $\tilde{\nu}$ = 2981 (s), 2871 (s), 1599 (s), 1567 (s) [$\nu_{\text{as}}(\text{CO})$], 1462 (s), 1426 (m), 1400 (s) [$\nu_{\text{s}}(\text{CO})$], 1359 (w), 1312 (w), 1238 (s) [$\nu(\text{SO}_3)$], 1211 (s), 1088 (s) [$\nu_3(\text{ClO}_4)$], 1030 (s), 976 (w), 918 (w), 828 (w), 781 (m), 763 (m), 742 (w), 697 (m), 653 (w), 622 (s) [$\nu_4(\text{ClO}_4)$], 566 (m), 525 (w), 499 (w), 426 (w) cm^{-1} .

Crystallography: Suitable crystals of compound **5b**(ClO₄)·MeCN and **7d**(BPh₄)·0.5MeCN·0.5H₂O were selected and mounted on the tip of a glass fiber (Table 6). The data sets were collected at 213(2) K using a STOE IPDS-2T diffractometer equipped with graphite-monochromated Mo- K_{α} radiation (0.71073 Å). The intensity data were processed with the program STOE X-AREA. An

Table 6. Crystallographic data for **5b**(ClO₄)·MeCN and **7d**(BPh₄)·0.5MeCN·0.5H₂O.

	5b (ClO ₄)·MeCN	7d (BPh ₄)·0.5MeCN·0.5H ₂ O
Formula	C ₄₇ H ₆₈ ClN ₇ Ni ₂ O ₆ S ₂	C ₆₃ H _{77.5} BN _{6.50} Ni ₂ O _{9.50} S ₂
M_r [g mol ⁻¹]	1044.07	1268.65
Space group	$P\bar{1}$	$C2/c$
a [Å]	12.7350(7)	36.727(3)
b [Å]	14.0924(7)	16.2006(13)
c [Å]	14.6442(8)	24.993(19)
α [°]	85.01(4)	90.00
β [°]	70.86(4)	115.484(8)
γ [°]	70.95(4)	90.00
V [Å ³]	2346.3(8)	13427.2(18)
Z	2	8
d_{calcd} [g cm ⁻³]	1.478	1.255
Crystal size [mm ³]	0.10 × 0.10 × 0.10	0.27 × 0.22 × 0.22
μ (Mo- K_{α}) [mm ⁻¹]	1.006	0.680
θ limits [°]	3.35–26.00	5.53–24.09
Measured reflections	23395	35779
Indep. reflections	9218	9930
Obsd. reflections ^[a]	8154	6430
Parameters	632	764
$R1$ ^[b] ($R1$ all data)	0.0632 (0.0699)	0.0482 (0.0723)
$wR2$ ^[c] ($wR2$ all data)	0.1644 (0.1672)	0.1238 (0.1306)
Max./min peaks	2.934/–2.577	0.641/–0.499
ρ [e Å ⁻³]		

[a] Observation criterion: $I > 2\sigma(I)$. [b] $R1 = \sum||F_o| - |F_c||/\sum|F_o|$. [c] $wR2 = \{\sum[w(F_o^2 - F_c^2)^2]/\sum[w(F_c^2)^2]\}^{1/2}$.

empirical absorption correction was performed with the program SADABS.^[49] Structures were solved by direct methods^[50] and refined by full-matrix least squares on the basis of all data against F^2 using SHELXL-97.^[51] PLATON was used to search for higher symmetry.^[52] Drawings were produced with Ortep-3.^[53] Hydrogen atoms were placed at calculated positions and refined as riding atoms with isotropic displacement parameters. All non-hydrogen atoms were refined anisotropically. In the crystal structure of **5b**[ClO₄]₄·MeCN the ClO₄⁻ ions was found to be disordered over two positions. A split-atom model has been used to account for this disorder using the AFIX 3 and EADP instructions implemented in the SHELXL program suite. The site-occupancy factors of the two orientations were refined as O3A–O6A/O3B–O6B = 0.60:0.40. In the crystal structure of **7d**[BPh₄]_{0.5}MeCN·0.5H₂O the occupancy factors of the MeCN and H₂O solvate molecules were fixed at 0.50. No hydrogen atoms were calculated for the solvate molecules.

CCDC-837598 (for **5b**) and -837599 (for **7d**) contain the supplementary crystallographic data for this paper. These data can be obtained free of charge from The Cambridge Crystallographic Data Centre via www.ccdc.cam.ac.uk/data_request/cif.

Acknowledgments

We are thankful to Prof. Dr. H. Krautscheid for providing facilities for X-ray crystallographic measurements. This work was supported by the Deutsche Forschungsgemeinschaft (DFG) (Graduate School “BuildMona”).

- [1] N. H. Pilkington, R. Robson, *Aust. J. Chem.* **1970**, *23*, 2225–2236.
- [2] a) A. J. Atkins, A. J. Blake, M. Schröder, *J. Chem. Soc., Chem. Commun.* **1993**, 1662–1665; b) N. D. J. Branscombe, A. J. Blake, A. Marin-Becerra, W.-S. Li, S. Parsons, L. Ruiz-Ramirez, M. Schröder, *Chem. Commun.* **1996**, 2573–2574.
- [3] a) S. Brooker, P. D. Croucher, *J. Chem. Soc., Chem. Commun.* **1995**, 1493–1494; b) S. Brooker, P. D. Croucher, *J. Chem. Soc., Chem. Commun.* **1995**, 2075–2076; c) S. Brooker, P. D. Croucher, F. M. Roxburgh, *J. Chem. Soc., Dalton Trans.* **1996**, 3031–3037; d) S. Brooker, P. D. Croucher, *Chem. Commun.* **1997**, 459–460.
- [4] A. J. Atkins, D. Black, A. J. Blake, A. Marin-Becerra, S. Parsons, L. Ruiz-Ramirez, M. Schröder, *Chem. Commun.* **1996**, 457–464.
- [5] a) S. Brooker, P. D. Croucher, T. C. Davidson, G. S. Dunbar, A. J. McQuillan, G. B. Jameson, *Chem. Commun.* **1998**, 2131–2132; b) D. J. E. Spencer, A. C. Marr, M. Schröder, *Coord. Chem. Rev.* **2001**, *219–221*, 1055–1074.
- [6] A. L. Gavrilova, C. Jin Qin, R. D. Sommer, A. L. Rheingold, B. Bosnich, *J. Am. Chem. Soc.* **2002**, *124*, 1714–1722.
- [7] a) S. Brooker, *Coord. Chem. Rev.* **2001**, *222*, 33–56; b) S. Brooker, P. D. Croucher, T. C. Davidson, G. S. Dunbar, C. U. Beck, S. Subramanian, *Eur. J. Inorg. Chem.* **2000**, 169–179.
- [8] C. D. Gutsche, *Calixarenes Revisited*, in: *Monographs in Supramolecular Chemistry* (Ed.: J. F. Stoddart), Royal Society of Chemistry, Cambridge, UK, **1998**.
- [9] B. Kersting, *Z. Anorg. Allg. Chem.* **2004**, *630*, 765–780.
- [10] V. Lozan, C. Loose, J. Kortus, B. Kersting, *Coord. Chem. Rev.* **2009**, *253*, 2244–2260.
- [11] V. Lozan, B. Kersting, *Inorg. Chem.* **2008**, *47*, 5386–5393.
- [12] U. Lehmann, J. Klingele, V. Lozan, G. Steinfeld, M. H. Klingele, S. Käss, A. Rodenstein, B. Kersting, *Inorg. Chem.* **2010**, *49*, 11018–11029.
- [13] B. Kersting, in *Activating Unreactive Molecules – The Role of Secondary Interactions* (Eds.: C. Bolm, F. E. Hahn), Wiley-VCH, Weinheim **2009**, pp. 1–17.
- [14] B. Kersting, U. Lehmann, *Adv. Inorg. Chem.* **2009**, *61*, 407–470.
- [15] G. Steinfeld, V. Lozan, B. Kersting, *Angew. Chem.* **2003**, *115*, 2363–2365; *Angew. Chem. Int. Ed.* **2003**, *42*, 2261–2263.
- [16] S. Käss, T. Gregor, B. Kersting, *Angew. Chem.* **2006**, *118*, 107–110; *Angew. Chem. Int. Ed.* **2006**, *45*, 101–104.
- [17] M. Gressenbuch, V. Lozan, G. Steinfeld, B. Kersting, *Eur. J. Inorg. Chem.* **2005**, 2223–2234.
- [18] M. Gressenbuch, B. Kersting, *Eur. J. Inorg. Chem.* **2007**, 90–102.
- [19] M. Gressenbuch, B. Kersting, *Dalton Trans.* **2009**, 5281–5283.
- [20] U. Lehmann, B. Kersting, unpublished results.
- [21] J. Hausmann, S. Käss, S. Klod, E. Kleinpeter, B. Kersting, *Eur. J. Inorg. Chem.* **2004**, 4402–4411.
- [22] M. Gressenbuch, B. Kersting, *Z. Anorg. Allg. Chem.* **2010**, 636, 1435–1437.
- [23] T. Gregor, C. F. Weise, V. Lozan, B. Kersting, *Synthesis* **2007**, 3706–3712.
- [24] B. Kersting, G. Steinfeld, *Chem. Commun.* **2001**, 1376–1377.
- [25] B. Kersting, *Angew. Chem.* **2001**, *113*, 4109–4112; *Angew. Chem. Int. Ed.* **2001**, *40*, 3987–3990.
- [26] The chemical formula of this compound is shown in Scheme 1.
- [27] All attempts to prepare a chlorido-bridged zinc complex [Zn₂L²(Cl)]⁺ invariably proved unsuccessful, as was also observed in the case of H₂L¹ in the literature.^[24]
- [28] J. Klingele, M. H. Klingele, O. Baars, V. Lozan, A. Buchholz, G. Leibeling, W. Plass, F. Meyer, B. Kersting, *Eur. J. Inorg. Chem.* **2007**, 5277–5285.
- [29] T. Glaser, Y. Journaux, G. Steinfeld, V. Lozan, B. Kersting, *Dalton Trans.* **2006**, 1738–1748.
- [30] M. Hesse, H. Meier, B. Zeeh, *Spektroskopische Methoden in der Organischen Chemie*, Thieme Verlag, Stuttgart, 5th ed., **1995**.
- [31] K. Nakamoto, *Infrared and Raman Spectra of Inorganic and Coordination Compounds*, 5th ed., Wiley, New York, **1997**.
- [32] G. B. Deacon, R. J. Philipp, *Coord. Chem. Rev.* **1980**, *33*, 227–250.
- [33] D. Martini, M. Pellei, C. Pettinari, B. W. Skelton, A. H. White, *Inorg. Chim. Acta* **2002**, *333*, 72–82.
- [34] A. B. P. Lever, O. Odgen, *J. Chem. Soc.* **1967**, 2041–2046.
- [35] K. Wieghardt, *J. Chem. Soc., Dalton Trans.* **1973**, 2548–2552.
- [36] M. Y. Darensbourg, T. Tuntulani, J. H. Reibenspies, *Inorg. Chem.* **1995**, *34*, 6287–6294.
- [37] The magnetic properties of these complexes are assumed to be similar to other carboxylato-bridged [Ni₂L¹(O₂CR)]⁺ complexes. The complexes are assumed to exhibit an $S = 2$ ground state as observed in [Ni₂L¹(OAc)]⁺ and [Ni₂L¹(O₂CPh)]⁺. See J. Hausmann, M. H. Klingele, V. Lozan, G. Steinfeld, D. Siebert, Y. Journaux, J. J. Girerd, B. Kersting, *Chem. Eur. J.* **2004**, *10*, 1716–1728.
- [38] A. B. P. Lever, *Inorganic Electronic Spectroscopy*, 2nd edition, Elsevier Science, Amsterdam, **1984**.
- [39] V. Lozan, B. Kersting, *Eur. J. Inorg. Chem.* **2005**, 504–512.
- [40] V. Lozan, B. Kersting, *Eur. J. Inorg. Chem.* **2005**, 504–512.
- [41] V. Lozan, A. Buchholz, W. Plass, B. Kersting, *Chem. Eur. J.* **2007**, *13*, 7305–7316.
- [42] C. Pedone, E. Benedetti, A. Immirzi, G. Allegra, *J. Am. Chem. Soc.* **1970**, *92*, 3549–3552.
- [43] H. R. Christen, *Grundlagen der Organischen Chemie*, 6th ed., Salle Verlag, Frankfurt/Main, Germany, **1985**, p. 233.
- [44] J. W. Steed, J. L. Atwood, *Supramolecular Chemistry*, 2nd ed., Wiley, Chichester, UK, **2009**.
- [45] F. A. Cotton, G. Wilkinson, C. A. Murillo, M. Bochmann, *Advanced Inorganic Chemistry*, 6th ed., Wiley-VCH, Weinheim, Germany, **1999**, p. 492.
- [46] The values for the dissociation constants were taken from: G. Kortüm, W. Vogel, K. Andrussov, *Pure Appl. Chem.* **1960**, *1*, 187–536.
- [47] J. Monnin, *Helv. Chim. Acta* **1958**, *41*, 2112–2119.
- [48] G. E. Dunn, R. S. McDonald, *Can. J. Chem.* **1969**, *47*, 4577–4588.

- [49] G. M. Sheldrick, *SADABS, Area-detector absorption correction*, University of Göttingen, Germany.
- [50] G. M. Sheldrick, *Acta Crystallogr., Sect. A* **1990**, *46*, 467–473.
- [51] G. M. Sheldrick, *SHELXL-97, Computer program for crystal structure refinement*, University of Göttingen, Göttingen, Germany, **1997**.
- [52] A. L. Spek, *PLATON: A Multipurpose Crystallographic Tool*, Utrecht University, Utrecht, The Netherlands, **2000**.
- [53] L. J. Farrugia, *J. Appl. Crystallogr.* **1997**, *30*, 565–568.

Received: January 13, 2012
Published Online: March 23, 2012